Role of Surface Intramolecular Dynamics in the Efficiency of Energy Transfer in Ne Atom Collisions with a *n*-Hexylthiolate Self-Assembled Monolayer†

Tianying Yan,‡ N. Isa,§ K. D. Gibson,§ S. J. Sibener,§ and William L. Hase*,‡

Department of Chemistry and Department of Computer Science, Wayne State University, Detroit, Michigan 48202, and Department of Chemistry, The James Franck Institute, The University of Chicago, Chicago, Illinois 60637

Received: April 24, 2003; In Final Form: September 16, 2003

The energy-transfer dynamics associated with Ne atom collisions with a *n*-hexylthiolate self-assembled monolayer (SAM) surface at 20 kcal/mol collision energy are studied in chemical dynamics simulations by using both harmonic/separable and anharmonic/coupled surface models and by considering a SAM in both its classical potential energy minimum and containing a 293 K energy distribution. For the anharmonic surface, excitation of higher-energy potential energy minima arising from different intermolecular conformations of the alkyl chains and intramolecular vibrational energy redistribution (IVR) between the surface modes during the collision enhance the energy transfer from Ne atom translation to the surface. IVR is efficient for the alkyl chain's torsional modes and intramolecular chain-bending modes and occurs on the time scale of the Ne atom collisions. It does not occur during the collisions for other modes, such as the higher-frequency intrachain CCC bends. This IVR between surface modes, during the collision, increases the number of modes coupled to the Ne atom's translational motion and enhances energy transfer to the surface. Whether modes promoting or not promoting IVR are initially excited depends on the surface site at which the Ne atom collides. The simulation indicates that the presence of these different energy-transfer dynamics for different surface sites is the origin of the bimodal energy-transfer distribution function $P(E_f)$. It is suggested that a large number of surface modes and chains coupled by IVR, for collisions at some surface sites, may create a sufficiently large bath to form a Boltzmann-like component in $P(E_f)$.

I. Introduction

In thermal and hyperthermal gas−surface collisions, a bimodal final translational-energy distribution $P(E_f)$ may be observed for the scattered projectile.[1,2] Often the two peaks are assigned to a low-energy trapping−desorption (TD) channel and a higher-energy inelastic scattering (IS) channel,[1,2] but this is not always a correct interpretation.[3−5] A bimodal $P(E_f)$ is observed in both computer simulations[3−5] and experiments[6] of Ne atoms scattering off of alkylthiolate self-assembled monolayer (SAM) surfaces, and as shown in Figure 1, good agreement is obtained between simulation and experiment. It is possible to fit the low-energy peak to the Maxwell−Boltzmann distribution function

$$P(E_f) = (k_b T_{s,eff})^{-2} E_f \exp\left(-\frac{E_f}{k_b T_{s,eff}}\right) \quad (1)$$

where $T_{s,eff}$ is different than the surface temperature T_s. This suggests that the Ne atoms are not thermally accommodated when they collide with the surface, which is supported by the finding from the trajectories that most of the Ne−SAM collisions are direct events with only one inner turning point (ITP) in the relative motion of the Ne atom with respect to the surface.[3] The standard paradigm is that the collision requires multiple inner turning points (MITPs) for a full accommodation of the incident particle's energy and complete thermalization prior to desorption.[7] Thus, instead of identifying the Ne−SAM $P(E_f)$ as one with TD and IS components, a more accurate description is one with a low-energy Boltzmann-like component (BC) and a high-energy non-Boltzmann (NB) component. Both of these latter components arise from inelastic scattering. Distributions of residence time for the interactions between the Ne atoms and the SAM surface have been presented previously

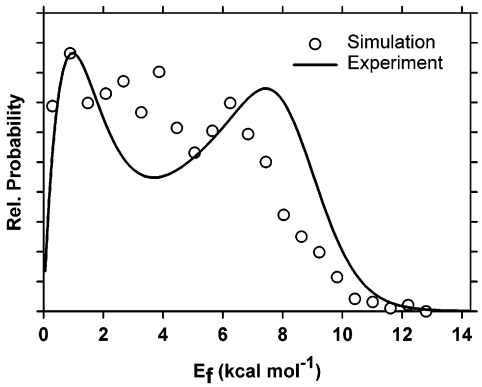

Figure 1. Comparison of simulation and experimental results of Ne atoms scattering off of a 1-decanethiolate SAM at $E_i = 12.7$ kcal/mol, $\theta_i = 45°$, and $T_s = 135$ K. The Ne atoms are colliding with a 15° azimuthal angle with respect to a plane defined by the ∼34° tilt angle of the thiolate chains. The SAM surface model is modeled with united-methyl and methylene groups on the thiolate chains self-assembled on a rigid Au{111} surface with periodic boundary conditions.

† Part of the special issue "Charles S. Parmenter Festschrift".

* To whom correspondence should be addressed. E-mail: wlh@cs.wayne.edu.

‡ Wayne State University.

§ The University of Chicago.

10.1021/jp035115e CCC: $25.00
Published on Web 10/31/2003

(i.e., Figure 4 in ref 3) for a range of incident energies and angles. The times range from 0.2 to 2 ps.

As shown in a previous study,[5] a bimoldal $P(E_f)$ is found in Ne−SAM simulations for a surface temperature T_s of 0 K. The low-energy component is Boltzmann-like and may be fit with an effective surface temperature $T_{s,eff}$ of 330 K, which is remarkably different from the actual surface temperature. As found for trajectory simulations with a higher T_s, a very small fraction of the trajectories have MITPS giving rise to a physisorbed Ne atom.[5] It is of fundamental interest to identify the energy-transfer pathways leading to the bimodal $P(E_f)$.

There are multiple pathways for translation-to-vibration (i.e., $T \rightarrow V$) energy transfer in gas−surface collisions. The structure of an alkylthiolate SAM with well-defined normal modes for the alkylthiolate chains but highly coupled anharmonic interchain modes is somewhat intermediate between that for a solid and that for a liquid. Mode−mode couplings are expected to be particularly important for the anharmonic interchain modes. Developing a complete and accurate model for Ne−SAM $T \rightarrow V$ energy-transfer processes requires identifying both the vibrational mode(s) initially excited by the collision and those excited by the subsequent relaxation of the SAM.

If intramolecular vibrational-energy redistribution (IVR)[8] for the SAM is faster than the residence time of the incident rare-gas atom, then efficient energy accommodation may occur, and a Boltzmann-like component may be present in $P(E_f)$. At low energies and low surface temperatures, IVR may be investigated by transforming the surface's Cartesian coordinates and momenta, used for solving the classical equation of motion, to normal-mode coordinates and momenta. Though this transformation is exact only in the small displacement limit,[9−11] it still gives realistic results if the total energy is not too large.[12] An alternative approach for studying energy-transfer mechanisms for gas−surface collisions is to use a Hamiltonian in which the surface motions are directly represented by normal modes.[13] The surface represented by this Hamiltonian is thus $3N - 6$ collective harmonic oscillators. Though this harmonic surface model does not allow mode−mode couplings and thus IVR, it allows one to study the surface modes initially excited by the impact of the projectile. Comparing the energy-transfer dynamics for the harmonic and anharmonic models provides information concerning the importance of IVR and conformational changes for the surface (i.e., properties present in the anharmonic model) for gas−surface energy transfer.

In the work presented here, the role of surface intramolecular dynamics in promoting energy transfer in Ne−SAM collisions is investigated. The computational method is briefly described in section II. Results for both the harmonic and anharmonic SAM model, with $T_s = 0$ K and no zero-point energy (ZPE), are given in section III. In section IV, intramolecular dynamics for the anharmonic model are studied for the higher surface temperature of 293 K. The important findings of this study are discussed in section V.

II. Computational Method

The models for the SAM potential and the Ne−SAM intermolecular potential were described previously.[14] The SAM consists of 35 *n*-hexylthiolate chains self-assembled on a stiff Au{111} surface, with the methyl and methylene groups of the chains represented by united atoms. This model, identified as UA-small/Au-1-stiff/Ne-V(UA),[5] has been shown to be adequate for studying the dynamics of Ne−SAM thermal collisional-energy transfer[5] and comparing with experiment.[6] The potential for the SAM model was developed by Hautman and Klein,[15] incorporating previous work by Jorgenson,[16] to represent important properties of the SAM's experimental structure[17] (i.e., the commensurate $\sqrt{3} \times \sqrt{3}R30°$ structure and the ~30° tilt angle). The dihedral potential for a single alkyl chain has trans(180°) ↔ gauche(120°) and trans(180°) ↔ cis(0°) barriers of 5.2 and 2.7 kcal/mol, respectively. In previous work,[5] a variety models for the Au{111} surface were used, including one with multiple Au layers and a thermal bath. This model gave the same energy-transfer dynamics as the stiff model used here. The adequacy of the stiff Au{111} model arises from the short collision time for the Ne−SAM interaction and the large number of vibrational modes associated with the SAM.

The classical trajectory simulations were carried out with the general chemical dynamics package VENUS.[18] Initial conditions for the trajectories were chosen so that the incident Ne atoms were randomly aimed within the central unit cell on the SAM's surface. The initial velocity vectors of the Ne atoms are parallel to the tilt angle of the alkanthiolate chains' backbone so that the incident angle θ_i and azimuthal angle χ_i are 34 and 0°, respectively. The collision energy E_i is 20 kcal/mol. An angle of 34° represents the range of angles studied experimentally,[6] and a bimodal energy distribution is observed at this angle. The energy-transfer dynamics depends on the incident angle, and normal energy scaling does not describe the results.[3] For example, the accommodation of the parallel component of E_i is similar to that for the normal component.[3,6]

Simulations are performed with the SAM surface in its potential energy minimum (i.e., a classical mechanical temperature of 0 K) and at a surface temperature T_s of 293 K. For the latter, zero-point energy (ZPE) is included in the surface's energy, and the energies for the surface vibrational modes were sampled from their quantum harmonic oscillator distributions (i.e., a quasiclassical normal-mode sampling method[12,19]). In previous work,[5] we have shown for the Ne−SAM system that quasiclassical normal-mode sampling and molecular dynamics classical mechanical sampling of the surface give the same trajectory results. The understanding of this finding is that for the short Ne−SAM collisions there is not sufficient time for zero-point energy to flow unphysically between the surface modes.[20,21] If not stated otherwise, the simulation results for a particular initial condition are based on 400 trajectories.

The above simulations assume that each Ne atom collision with the surface is an isolated event. This is the situation for the experiments of Sibener's research group, with which the simulations are compared. In the experimental setup, one Ne atom hits a unit-cell at approximate intervals of several hundred picoseconds.

III. Simulation Results

A. Harmonic and Anharmonic Surface Models with $T_s = 0$ K. *1. Energy-Transfer Pathways. Average Energies versus Time.* The total energy for the Ne−SAM system may be written as

$$E_{total} = T_{Ne} + V_{Ne-Surf} + E_{surf} \quad (2)$$

where T_{Ne} is the Ne translational energy, $V_{Ne-Surf}$ is the intermolecular potential energy between Ne and the SAM surface, and E_{surf} is the sum of the surface potential and kinetic energies. Average values for these three energies versus time were determined for Ne atoms colliding with both the harmonic and anharmonic SAM surfaces at $T_s = 0$ K with no ZPE. The results are plotted in Figure 2a and b for the anharmonic and harmonic models, respectively. The average energies for the

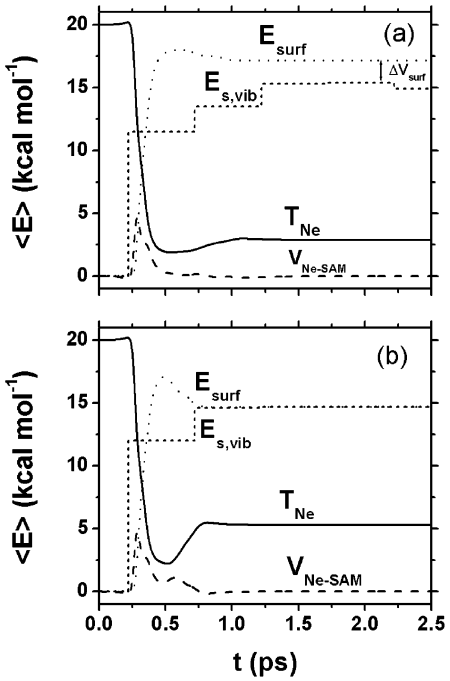

Figure 2. Average energy vs time. E_{surf}, total surface energy; $E_{s,vib}$, surface vibrational energy; T_{Ne}, Ne atoms' kinetic energy; V_{Ne-SAM}, Ne−SAM intermolecular potential energy; and ΔV_{surf}, conformational energy of SAM. (a) Anharmonic SAM; (b) harmonic SAM.

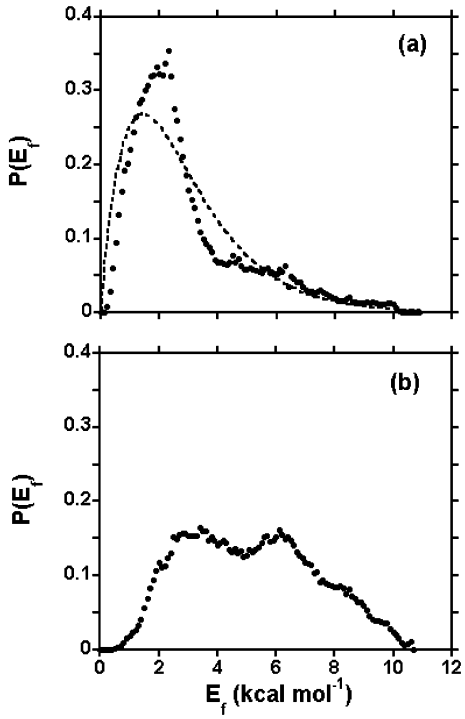

Figure 3. Final translational-energy distribution $P(E_f)$ for Ne atoms scattering off of a SAM surface. Initial conditions are $E_i = 20$ kcal/mol, incident along the SAM tilt direction, and $T_s = 0$ K without ZPE. (a) Anharmonic SAM; (b) harmonic SAM.

harmonic model, which become constant at ∼0.75 ps, show that the average collision lasts about 0.5 ps, consistent with residence times that range from 0.2 to 1 ps.[3] For the first 0.5 ps of the simulation, the average energies for the two surfaces are very similar. However, as expected, the Ne atoms scattering off of the harmonic surface experience a stiffer surface and rebound with a higher average translational energy $\langle E_f \rangle$. The surface energy E_{surf} is more elastic for the harmonic surface. Eighty-five and 73% of the initial Ne atoms' translational energy is transferred to the anharmonic and harmonic surfaces, respectively.

Additional understanding of the pathways for energy transfer to the SAM is obtained by calculating the average surface vibrational energy, $E_{s,vib}$, versus time. Because the SAM's normal-mode kinetic energy is well defined for both the anharmonic and harmonic surface models,[13] $E_{s,vib}$ was obtained from the maxima of the kinetic energies of the normal modes and is given by

$$E_{s,vib}(t \rightarrow t + \Delta t) = \sum_{i=1}^{3N-6} E_i(t \rightarrow t + \Delta t) = \sum_{i=1}^{3N-6} \langle T_i^{max}(t \rightarrow t + \Delta t) \rangle = \sum_{i=1}^{3N-6} \left[\frac{1}{M_j} \sum_{jj=1}^{M_j} T_i^{j,max}(t \rightarrow t + \Delta t) \right] \quad (3)$$

where N is the number of surface atoms, $t \rightarrow t + \Delta t$ is the time interval, and M_j is the number of maxima in the interval for all of the trajectories, and $\Delta t = 0.5$ ps. For the harmonic surface model, $E_{s,vib}$ and E_{surf} become equivalent after the Ne atom scatters, which is the required result for the harmonic model. However, for the anharmonic surface model, $E_{s,vib}$ and E_{surf} are not the same immediately after the collision. Thus, the Ne atoms import additional energy to the surface besides the excitation of the surface's vibrational modes. For the anharmonic model, energy may also be deposited in the surface by exciting higher-energy potential energy minima (i.e., conformations) of the SAM (see discussion below). This conformational potential energy is denoted ΔV_{surf}. This additional channel for energy transfer may explain why the anharmonic surface adsorbs more of the collision energy. However, additional studies/tests are needed to determine if this is indeed the case.

Figure 2a shows that at the end of the simulation, where $t = 2.5$ ps and ΔV_{surf} is identified as the difference between E_{surf} and $E_{s,vib}$, ΔV_{surf} is 2−2.5 kcal/mol and 10−15% of the surface energy. For a cold, larger surface model, the SAM is expected to relax to its equilibrium conformation at long time so that ΔV_{surf} becomes zero. For this study, the surface is not of sufficient size (i.e., insufficient number of alkyl chains) and the numerical integration is not long enough to study this $\Delta V_{surf} \rightarrow E_{s,vib}$ relaxation. This is not a consequence of comparing a simulated 6-carbon chain with the experimental 10-carbon chain data; the results herein essentially converge to the 6-carbon atom limit.[6]

2. Final Translational-Energy Distribution of the Scattered Ne Atoms. The final translational-energy distribution, $P(E_f)$, for the Ne atoms scattering off of the SAM is shown in Figure 3a and b for the anharmonic and harmonic surface models, respectively. Both distributions are determined from 1000 trajectories with exactly the same initial conditions. Because the SAM surface is static at the beginning of each trajectory and is excited only through the Ne atom's collisions, the differences in energy transfer for the trajectories for each surface arise from the Ne atoms striking different places on the surface's unit cell.

For both surfaces, $P(E_f)$ is bimodal, which is more pronounced for the harmonic surface. Apparently, the anharmonic surface has an additional mechanism (or mechanisms) for energy

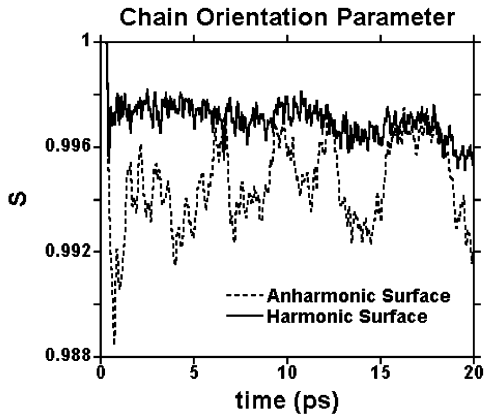

Figure 4. Chain orientation parameter of the anharmonic and harmonic SAM surfaces after collision with a Ne atom.

transfer, increasing the low-energy component of $P(E_f)$. For the anharmonic surface, this low-energy component is only approximately Boltzmann. The fit of the anharmonic surface $P(E_f)$ with eq 1 is given in Figure 3a. The effective temperature for the fit is 718 K. For a quasiclassical model for the SAM at 0 K but with ZPE included, the low-energy component is well fit by eq 1.[5] As shown below, the anharmonic surface has two pathways for energy transfer, which are not present for the harmonic surface. They are conformational changes of the alkyl chains comprising the SAM and intramolecular vibrational energy redistribution (IVR) between the SAM's vibrational modes during the Ne atoms' collisions. The latter has the effect of coupling more surface modes with the Ne atom's translational motion.

The bimodal energy distribution for the harmonic surface must arise from different efficiencies for energy transfer to the SAM when the colliding Ne atoms strike different places on the surface's unit cell. For collisions with certain surface regions, modes may be easily excited, and efficient energy transfer occurs. However, if the Ne atom strikes other positions, then the energy transfer may be very inefficient. Similar energy-transfer dynamics may also occur for the anharmonic surface. Therefore, a bimodal $P(E_f)$ distribution might be an intrinsic property of Ne−SAM collisions for both thermal and hyperthermal incident energy.

3. Chain Orientation Parameter of the SAM Surface. A MD simulation of the anharmonic SAM surface at $T_s = 300$ K shows there are dramatic trans → gauche (t → g) conformational changes, especially for the terminal methyl group;[15] t → g is not observed in this simulation of Ne−SAM collisions at $T_s =$ 0 K. Initially, the surface has no energy, and the total system energy is only the incident Ne atom's energy of 20 kcal/mol, so the likelihood is very low that the available energy is directed to a torsion by a collision leading to a t → g conformational change. However, conformational changes may still be induced through reorientations of the multiple alkyl chains from their equilibrium configurations. The chain orientation parameter for the SAM was determined from[22]

$$S = \left\langle \frac{1}{2}(3\cos^2 \vartheta_i - 1) \right\rangle \qquad (4)$$

where ϑ_i is the angle between ith sub-bond vector and the equilibrium chain backbone.

The time evolution of the chain orientation parameter for the anharmonic and harmonic surface models is shown in Figure 4. The calculation for each surface is based on a single trajectory. The harmonic surface allows only one configuration. The SAM

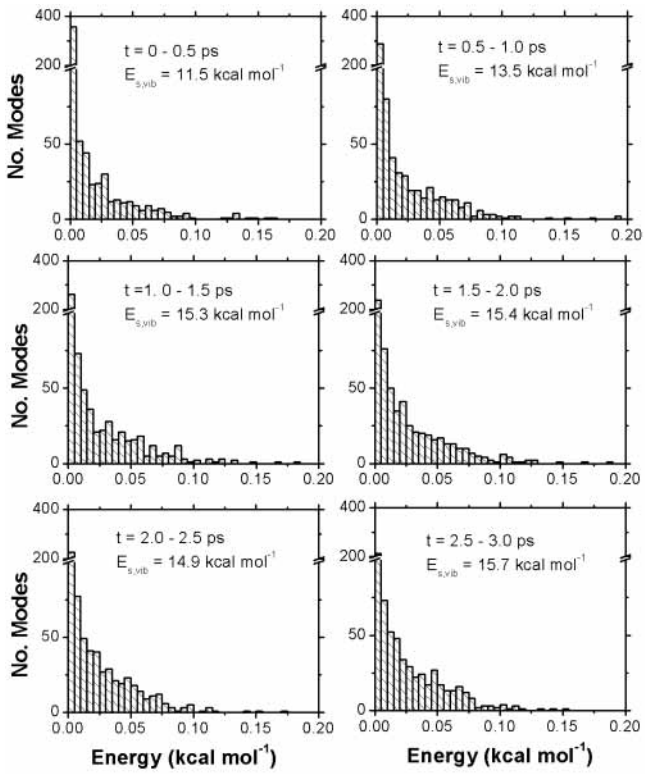

Figure 5. Distribution of energy (kcal/mol) in the vibrational modes of the SAM vs time (ps) for 0.5-ps time intervals. Results are for the anharmonic surface model.

vibrates about its global potential minimum with only small changes in its chain orientation parameter. In contrast, the anharmonic SAM surface model traverses a much more extensive region of configuration space, even at very short times as the Ne atom collides. The oscillation of the anharmonic surface's chain orientation parameter indicates that the surface resides in different local potential energy minima for times of 1 ps or more. The anharmonic SAM surface retains a certain amount of potential energy that is not released to surface vibrational energy, $E_{s,vib}$, during the simulation. Collision-induced conformational changes are important in the energy-transfer dynamics of Ne−SAM scattering.

4. Mode−Mode Couplings and Intramolecular Vibrational Dynamics. Intramolecular energy transfer occurs between the vibrational modes of the anharmonic surface model during and after the Ne atom's collision. The distribution of energies in the SAM's vibrational modes versus time is plotted in Figure 5, where time zero is defined as the time when one surface vibrational mode acquires more than 1 cm^{-1} of energy. Results are given for 0.5-ps time intervals out to 3.0 ps. The fraction of modes that are in the low-energy intercept of the distribution decreases from ∼50% for the 0−0.5-ps interval to ∼30% for the 2.5−3.0-ps interval. Thus, with increases in time the fraction of the modes with negligible excitation decreases. The simulations were carried out to 5 ps, and for times between 3 and 5 ps, there are only small changes in the distribution of energy in the surface modes and $E_{s,vib}$ varies between 15.5 and 15.7 kcal/mol.

The time-dependent distributions of energy in the modes of the harmonic SAM surface are not shown. For the 0−0.5- and 0.5−1.0-ps time intervals, they are very similar to those in Figure 5 for the anharmonic surface. $E_{s,vib}$ values for the two respective time intervals are 12.0 and 14.6 kcal/mol for the harmonic surface and are similar to the values of 11.5 and 13.5

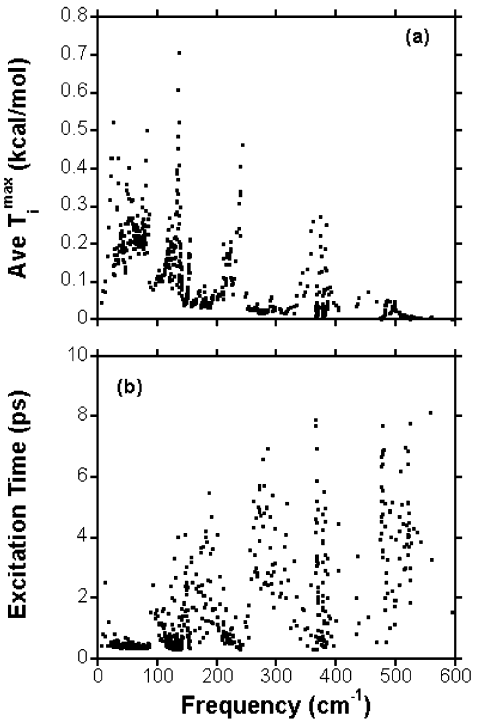

Figure 6. (a) Maximum kinetic energy acquired by a vibrational mode of the SAM, during a 5-ps trajectory, averaged over 400 trajectories. $\langle T_i^{max} \rangle$ is plotted versus the frequency of mode *i*. (b) Time for a vibrational mode of the SAM to acquire a kinetic energy of 1 cm^{-1}, averaged over 400 trajectories.

kcal/mol in Figure 5 for the anharmonic surface (i.e., these average $E_{s,vib}$ values may also be obtained from Figure 2 for the two time intervals). Because IVR does not occur between the modes of the harmonic SAM surface after the Ne atom scatters, the energy distribution for the modes of the harmonic surface do not change after the 0.5−1.0-ps time interval.

If there is efficient IVR between the vibrational modes of the SAM, then the average energies of the SAM's vibrational modes will be nearly the same. Though average oscillator energies are identical for a collection of classical harmonic oscillators with a statistical energy distribution, there will be small differences in the average energies if the oscillators are anharmonic.[23] To study the extent of IVR for the SAM, the maximum kinetic energy acquired by each vibrational mode of the SAM during the 5.0-ps motion of the SAM after the Ne atom's impact was determined for each trajectory. An average maximum kinetic energy for mode *i*, $\langle T_i^{max} \rangle$, was then determined by averaging the T_i^{max} value for each trajectory over 400 trajectories. The results are striking and are given in Figure 6a, where $\langle T_i^{max} \rangle$ is plotted versus the frequency of mode *i*. The excitation of the modes is not stochastic because some modes are preferentially excited over others. The preferential excitation is not restricted to a particular frequency range, though the modes with frequencies below 90 cm^{-1} tend to be more highly excited. The origin of the peaking in $\langle T_i^{max} \rangle$ at frequencies of approximately 26, 83, 135, 240, and 380 cm^{-1} is interesting but not fully resolved. The modes with the largest $\langle T_i^{max} \rangle$ for these approximate frequencies correspond to intermolecular bending of multiple chains for ν of 26 and 83 cm^{-1} and localized CCC bending of 1−3 chains for ν of 135, 240, and 380 cm^{-1}. There are broad frequency ranges for which there is no appreciable excitation of the modes.

The modes of the SAM may receive energy on different time scales. This is illustrated in Figure 6b for a 10-ps simulation

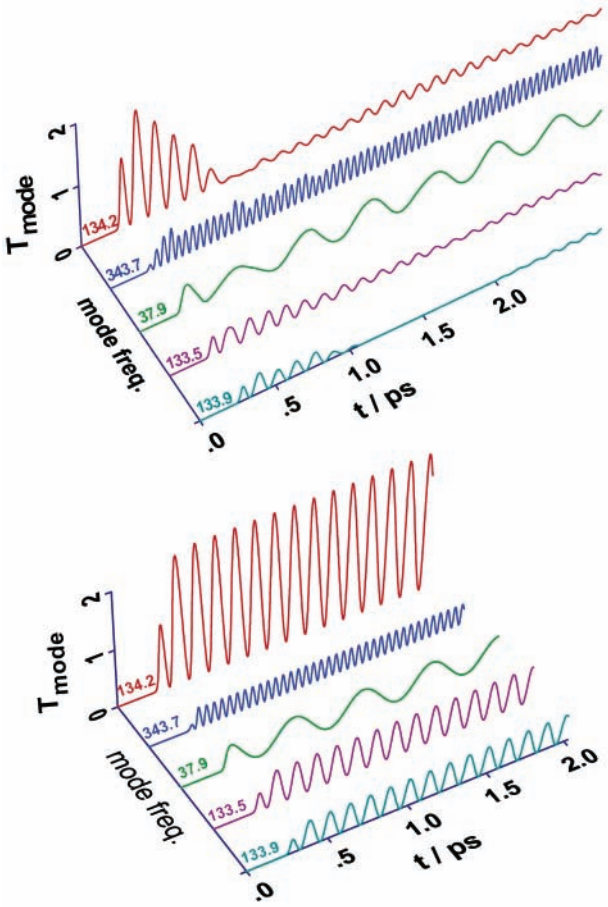

Figure 7. Evolution of the kinetic energy vs time for the five highest excited modes of a trajectory with inefficient energy transfer. Results are shown for the anharmonic (top plot) and harmonic (bottom plot) surface models. For each, the Ne atom is aimed at the same site on the surface unit cell. The initial surface temperature is 0 K, without ZPE, and the incident Ne atom energy is 20 kcal/mol.

study, where the time required for mode *i* to acquire a kinetic energy of $T_i \geq 1$ cm^{-1} is averaged over 400 trajectories. Some modes receive this small amount of energy nearly instantaneously as the Ne atom collides, whereas for others the time is on the order of 10 ps. A comparison of Figure 6a and b shows that if a low-frequency mode has a large $\langle T_i^{max} \rangle$ then it tends to receive a small amount of energy in a very short period of time.

Intramolecular energy transfer between the vibrational modes of the SAM during the collision may enhance energy transfer from Ne translation to surface vibration. This is illustrated in Figures 7 and 8, where the time evolution of the kinetic energy for the five most highly excited surface modes is shown for two trajectories with inefficient and efficient energy transfer. In each Figure, the results of a trajectory are shown for collision with both the anharmonic and harmonic surface models. For each surface, the Ne atom is aimed at the same site on the surface unit cell. For Figure 7, the Ne atom collides with a site that gives inefficient energy transfer, whereas in Figure 8 the collision is with a site that gives efficient energy transfer. For the collision with the surface site that gives inefficient energy transfer (Figure 7), the energy of the scattered Ne atom is very similar for the anharmonic and harmonic surfaces (i.e., 9.77 and 9.98 kcal/mol, respectively). In contrast, the scattered Ne atom's energy is much different (i.e., 0.84 and 4.24 kcal/mol) for the anharmonic and harmonic surfaces, respectively, when it collides with the site that gives efficient energy transfer (Figure 8).

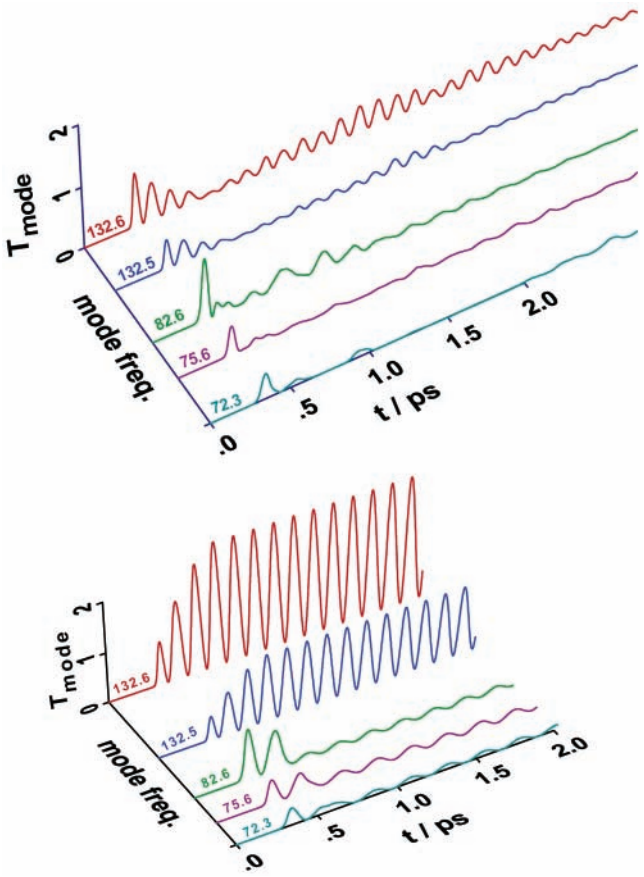

Figure 8. Same as Figure 7, except that the Ne atom is aimed at a site on the surface unit cell for which there is efficient energy transfer.

For the trajectories in both Figures 7 and Figure 8, the initial kinetic energy in each of the five modes is very similar for the anharmonic and harmonic surface models. For collision with the surface site that gives inefficient energy transfer (Figure 7), the kinetic energies of the modes versus time for the harmonic surface model show that the collision lasts ~0.2−0.3 ps. The mode energies are very similar for the two surface models during this time period as the collision occurs. However, at longer times some of the modes for the anharmonic surface lose energy through IVR processes. Figure 8 shows that the anharmonic and harmonic surfaces give much different energy-transfer dynamics for Ne atom collision with the surface site that gives efficient energy transfer. The kinetic energies for the modes of the harmonic surface show that the collision lasts ~0.4 ps. In the initial stage of the collision, the mode energies for the two surfaces are similar. However, as the collision proceeds the modes of the harmonic surface continue accumulating energy, and the modes of the anharmonic surface lose energy, redistributing it to other surface modes. The implication is that the coupling between modes and IVR during the collision for the anharmonic surface enhances energy transfer to the surface so that the scattered Ne atom's energy is 0.84 kcal/mol and much smaller than the 4.24 kcal/mol value for the harmonic surface.

The trajectory with efficient energy transfer excites different types of surface modes than does the one with inefficient energy transfer. The modes excited in Figure 7 for the trajectory with inefficient energy transfer are alkylthiolate chains collective wagging (37.9), CCC bending (133.5, 133.9, and 134.2), and vertical vibration of alkylthiolate chains (343.7). Except for the 37.9-cm^{-1} mode, these are modes for intramolecular motions of the chains. For the trajectory in Figure 8 with efficient energy transfer, the modes excited are CCC torsions of the alkylthiolate chains (72.3), symmetric bending of chain rows (75.6), asymmetric bending of chain rows (82.6), and CCC torsions and wagging of central chains (132.5 and 132.6). These modes are composed of CCC torsions and intermolecular bending of multiple chains. The suggestion, from comparing the types of modes excited by the trajectories giving inefficient and efficient energy transfer, is that energy is retained in the intramolecular CCC bending and stretching modes of the alkyl chains for a relatively long time and IVR is slow. In contrast, the excitation of CCC torsion and intermolecular modes by trajectories with efficient energy transfer gives rise to efficient IVR during the collision and a large "bath" of surface modes coupled to the Ne atom translational motion.

B. Anharmonic Surface Model with T_s = 293 K. In the above simulations, energy transfer to the SAM surface and the surface's intramolecular dynamics were studied for a surface initial condition of $T_s = 0$ K and no zero-point energy. To study the effect of increasing the surface temperature, simulations were also performed for an initial surface temperature of 293 K, with zero-point energy added by the quasiclassical method as described in section II. The above simulation, at $T_s = 0$ K and without zero-point energy, has a low surface energy, and normal-mode coordinates are meaningful for studying how energy is deposited in the surface and transferred between surface modes. However, for the much higher surface energy for the quasiclassical simulation at $T_s = 293$ K, the surface's normal-mode coordinates are less representative of the surface's vibrational motion,[9] and another approach is needed to investigate the surface intramolecular dynamics. The one used here is to study the relaxation of the autocorrelation function (ACF) for different types of surface modes.

1. Autocorrelation Function (ACF) for Different Types of Surface Modes. To study the intramolecular vibrational dynamics of the SAM at 293 K, a molecular dynamics trajectory was calculated for the SAM at this temperature. An autocorrelation function, defined by[24]

$$C(t) = \frac{\langle \phi(0) \cdot \phi(t) \rangle - \langle \phi(0) \rangle^2}{\langle \phi(0)^2 \rangle - \langle \phi(0) \rangle^2} \qquad (5)$$

was determined for both the CCC bending and torsional modes of the SAM. The CCC stretching modes are not significantly excited by the SAM, and their ACF was not considered. In eq 5, $\phi(t)$ are values for the bending (or torsional) angles at times 0 and t, and $\langle \phi(0) \rangle$ is the average value for the angles at $t = 0$. The ACF is evaluated by extracting values of ϕ at 10 000 equally spaced time intervals of a 100-ps trajectory. With this 0.01-ps sampling time interval, the simulation is able to resolve frequencies of $f_c = {}^1/_2\Delta = 50$ ps^{-1} = ~1666 cm^{-1} and lower by a discrete Fourier transform of $C(t)$.[25] Because the vibrational modes of the SAM excited by the Ne atom collision have frequencies much lower than 1666 cm^{-1}, the MD simulation and the ACFs describe the intramolecular dynamics of the modes participating in collision-energy transfer to the SAM.

Figure 9 shows that the relaxation of the bending modes is much slower than that for the torsional modes. The ACF for the bending modes oscillates between positive and negative values, indicating that the individual CCC angles oscillate around their equilibrium values, with weak couplings. The relaxation is slow, and the bending modes retain the memory of their initial conditions for more than 2 ps. In contrast, relaxation is rapid for the torsional modes and occurs on a 0.5-ps time scale, which is similar to the time for the Ne atom's collision with the surface (Figures 7 and 8). Thus, if torsional

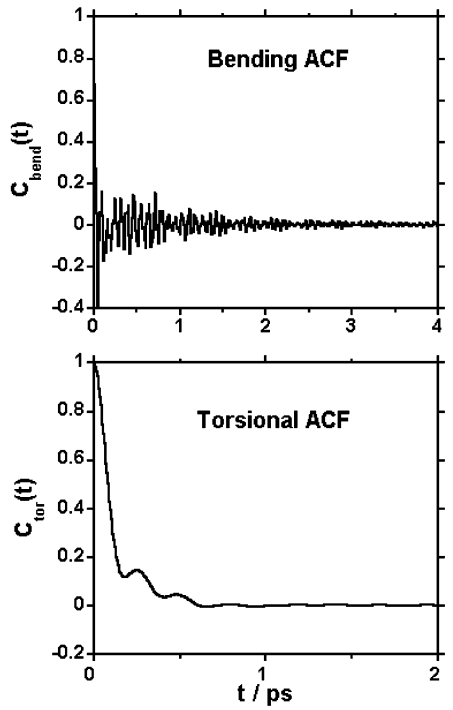

Figure 9. Autocorrelation function (ACF) at $T_s = 293$ K for the CCC bending (a) and torsion (b) angles.

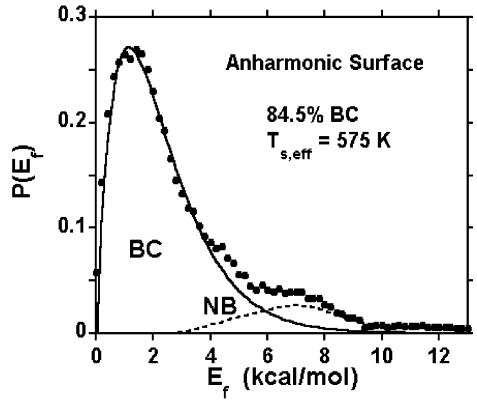

Figure 10. $P(E_f)$ of Ne atoms scattered off of the SAM surface at $T_s = 293$ K; BC, Boltzmann component; NB, non-Boltzmann component. The Boltzmann component has an effective temperature of 575 K.

modes are initially excited by the Ne atom's collision with the SAM, then IVR is expected to be rapid between the torsional modes and compete with the atom's residence on the surface. Such a bath of modes coupled to the Ne atom's translational motion during the collision may have the effect of "thermalizing" the Ne atom's translational energy and forming a Boltzmann-like component in its final translational-energy distribution.

2. Final Translational-Energy Distribution of the Scattered Ne Atoms. The final translational-energy distribution, $P(E_f)$, for Ne atoms scattered off of the 293 K SAM surface is shown in Figure 10. The average final energy $\langle E_f \rangle$ equals 2.98 ± 0.16 kcal/mol, which is much higher than the surface thermal energy of $2k_bT_s = 1.2$ kcal/mol. The $P(E_f)$ distribution may be deconvoluted into Boltzmann-like (BC) and non-Boltzmann (NB) components,[4] which comprise 84.5 and 15.5% of the distribution, respectively. The effective surface temperature $T_{s,eff}$ for the Boltzmann-like component is 575 K and is much higher than the surface temperature of 293 K.

The average total SAM surface energy with quasiclassical sampling at 293 K is 1400 kcal/mol. According to linear response theory,[26] the incident Ne atom's energy of 20 kcal/mol constitutes a small disturbance of the SAM's equilibrium energy distribution and therefore may merge with the surface's thermal motion. Because the system cannot distinguish whether such a distribution is caused by its own spontaneous fluctuation or by an incident Ne atom, the relaxation of the system following this distribution should coincide with the ACF for the system as described above. The residence time of Ne atoms on the surface is approximately 0.2−0.5 ps, which is on the same time scale as relaxation of the torsional and low-frequency interchain vibrational modes. Therefore, efficient energy accommodation, through fast IVR processes during the collision, is expected for collisions that excite these modes. However, less efficient energy accommodation may occur if only a small set of modes with slow IVR are excited during the Ne−SAM collision. The types of surface modes that are excited depend on the surface site with which the Ne atom collides, and the two types of energy transfer and accommodation dynamics should contribute to the bimodal $P(E_f)$.

IV. Summary

In the work reported here, the intramolecular dynamics of the surface is investigated to study the efficiency of energy transfer in collisions of Ne atoms with the *n*-hexylthiolate self-assembled monolayer (SAM) surface. Important components of the study are the use of both anharmonic/coupled and harmonic/separable models for the surface's vibrational modes and considering a surface at 0 K with no zero-point energy and one at 293 K with zero-point energy. The anharmonic surface has two energy-transfer mechanisms that are not present for the harmonic surface, which may enhance energy transfer from Ne atom translation to the surface. They are (1) the excitation of higher-energy potential energy minima arising from different intermolecular conformations of alkyl chains and (2) intramolecular vibrational energy redistribution (IVR) between the surface modes as the Ne atom collides.

For Ne atom collisions with the SAM at a collision energy of 20 kcal/mol, 10−15% of the collision energy is transfer to conformational potential energy, ΔV_{surf}, for higher-energy potential energy minima. For a cold surface, this ΔV_{surf} will relax to vibrational energy about the surface's global potential energy minimum. However, the surface model used here is not large enough to study this relaxation process. The time dependence of the chain orientation parameter for the alkyl chains indicates that after the Ne atom collision the alkyl chains reside in and move through different local potential energy minima. The relaxation of ΔV_{surf} to surface vibrational energy may be nonexponential.

IVR between surface modes as the Ne atom collides increases the number of modes to which the Ne atom translational motion is coupled and is expected to enhance energy transfer to the surface. IVR is rapid and occurs during the collision for the torsional modes of the alkyl chains and interchain bending modes. However, IVR is slower and does not occur during the collision for the intrachain CCC bending modes. The types of modes that are excited depend on the surface site at which the Ne atom collides. For some surface sites, multiple modes may be excited by IVR during the collision, leading to efficient energy transfer. Inefficient energy transfer may result if only a small number of modes, which do not undergo IVR during the collision, are excited. It is suggested that these different types of collisional energy-transfer efficiencies and dynamics for

different surface sites give rise to the bimodal Ne atom translational energy distribution $P(E_f)$.

Though an insignificant number of the Ne atom collisions have multiple inner turning points in the Ne + SAM relative motion (i.e., a property indicative of a collision intermediate), the Boltzmann-like component in $P(E_f)$ arising from efficient energy transfer may be fit by an effective surface temperature, $T_{s,eff}$, that is different from the actual surface temperature. The simulations indicate that a bath of surface modes, coupled via IVR for collision with some surface sites, allows the relatively small Ne atom translational motion to couple with a large vibrational heat bath as though it were a canonical system. Such energy-transfer dynamics has been discussed in the context of unimolecular rate theory.[27] Here, the canonical and microcanonical average translational energy of an atom dissociating from a polyatomic molecule, with a large vibrational heat bath, is $k_bT^* = E_{avl}/s$, where E_{avl} is the energy available for redistribution among the modes, s is the number of oscillators in the vibrational heat bath, and T^* is the product temperature and not necessarily the same as the system temperature T_s. The model proposed here of projectile translation coupled to multiple surface vibrational modes has some similarities to the model that couples projectile translation to multiple surface electronic states.[28]

The Boltzmann-like component in $P(E_f)$ arises from Ne atom collision with a surface not at 0 K, without zero-point energy, but with a surface with a finite temperature (e.g., 293 K). The SAM's thermal motion is expected to lead to more energy-transfer pathways when the Ne atom collides, leading to a broadened $P(E_f)$ distribution. A similar broadening in distributions associated with energy-transfer dynamics, as a system is energized above its classical potential energy minimum, was observed in a recent study[29] of vinylcyclopropane intramolecular and unimolecular dynamics.

Several future studies are suggested by the work presented here. It would be of interest to study IVR among the SAM's modes in more detail. Because IVR is achieved by mode−mode couplings, a study of the cross-correlation matrix[30] of normal-mode evolutions in time might identify mode−mode couplings and energy-transfer pathways. Additional information about the role of IVR between the SAM's modes and conformational changes of the SAM, in promoting the transfer of Ne atom translational energy to the SAM, may be determined by detailed calculations of the energy-transfer distribution $P(E_f)$ as a function of the surface collision site. Both the anharmonic and harmonic surface models could be used for this study. For some collision sites, the two models may give similar results, but for others, $P(E_f)$ will be strikingly different. Conformational changes for the SAM and IVR during the collision are expected to be important for these latter sites.

Additional studies are also suggested by a related simulation of Ne atom collisions with the 1-decanethiol SAM.[6] This work shows that the colliding Ne atom initially has direct contact with either the terminal methyl group of only one chain or terminal groups of two chains, depending on the collision site on the unit cell. For some collisions, multiple chains are excited during the collision, but for other collisions, the excitation is localized with only 1−2 chains initially excited. The suggestion from the current simulation presented here is that efficient energy transfer tends to be associated with the excitation of multiple chains and that there is a propensity for inefficient energy transfer with the excitation of only a small number of chains. These conjectures may be probed in future studies utilizing both the anharmonic and harmonic surface models. An important property to be determined in future work[31] is an "energy-transfer grid" identifying the efficiency of energy transfer at each impact point of the unit cell. It is expected that this grid will depend on the collision energy, incident angle, and azimuthal angle.

Acknowledgment. This work was primarily supported by the AFOSR-sponsored MURI center for Material Chemistry in the Space Environment. Supplemental support from the National Science Foundation − Material Research Science and Engineering Center at the University of Chicago is also gratefully acknowledged. T.Y.'s and W.L.H.'s participation in the project was also partially supported by the National Science Foundation. T.Y. thanks Dr. Samy Meroueh for many helpful discussions.

References and Notes

(1) Saecker, M. E.; Govoni, S. T.; Kowalski, D. V.; King, M. E.; Nathanson, G. M. *Science* **1991**, *252*, 1421.
(2) Shuler, S. F.; Davis, G. M.; Morris, J. R. *J. Chem. Phys.* **2002**, *116*, 9147.
(3) Yan, T.; Hase, W. L. *Phys. Chem. Chem. Phys.* **2000**, *2*, 901.
(4) Yan, T.; Hase, W. L.; Barker, J. R. *Chem. Phys. Lett.* **2000**, *329*, 84.
(5) Yan, T.; Hase, W. L. *J. Phys. Chem. B* **2002**, *106*, 8029.
(6) Isa, N.; Gibson, K. D.; Yan, T.; Hase, W. L.; Sibener, S. J. *J. Chem. Phys.*, submitted for publication, 2003.
(7) Head-Gordon, M.; Tully, J. C.; Rettner, C. T.; Mullins, C. B.; Auerbach, D. J. *J. Chem. Phys.* **1991**, *94*, 1516.
(8) *Advances in Classical Trajectory Methods: Intramolecular and Nonlinear Dynamics*; Hase, W. L., Ed.; JAI: London, 1992; Vol. 1.
(9) Wilson, E. B.; Decius, J. C.; Cross, P. C. *Molecular Vibrations*; McGraw-Hill: New York, 1955.
(10) Califano, S. *Vibrational States*; Wiley: New York, 1976.
(11) Flygare, W. F. *Molecular Structure and Dynamics*; Prentice Hall: Englewood Cliffs, NJ, 1978.
(12) Hase, W. L.; Ludlow, D. M.; Wolf, R. J.; Schlick, T. *J. Phys. Chem.* **1981**, *85*, 958.
(13) Yan, T.; Hase, W. L. *J. Phys. Chem. A* **2001**, *105*, 2617.
(14) Bosio, S. B. M.; Hase, W. L. *J. Chem. Phys.* **1997**, *107*, 9677.
(15) Hautman, J.; Klein, M. L. *J. Chem. Phys.* **1989**, *91*, 4994.
(16) Jorgenson, W. L. *J. Phys. Chem.* **1986**, *90*, 6379.
(17) Camillone, N., III.; Chidsey, C. E. D.; Eisenberger, P.; Fenter, P.; Li, J.; Lian, K. S.; Liu, G.-Y.; Scoles, G. *J. Chem. Phys.* **1993**, *99*, 744.
(18) Hase, W. L.; Duchovic, R. J.; Hu, X.; Kormonicki, A.; Lim, K.; Lu, D.-H.; Peslherbe, G. H.; Swamy, K. N.; Linds, S. R. V.; Varandos, A. J. C.; Wang, H.; Wolf, R. J. *QCPE* **1996**, *16*, 671.
(19) Chapman, S.; Bunker, D. L. *J. Chem. Phys.* **1975**, *62*, 2890.
(20) Lu, D.-h.; Hase, W. L. *J. Chem. Phys.* **1988**, *89*, 6723.
(21) Miller, W. H.; Hase, W. L.; Darling, C. L. *J. Chem. Phys.* **1989**, *91*, 2863.
(22) Fujiwara, S.; Sato, T. *J. Chem. Phys.* **1997**, *107*, 613.
(23) Hase, W. L.; Wolf, R. J.; Sloane, C. S. *J. Chem. Phys.* **1979**, 2911.
(24) Parker, M. E.; Heyes, D. M. *J. Chem. Phys.* **1998**, *108*, 9039.
(25) Press, W. H.; Teukolsky, S. A.; Vetterling, W. T.; Flannery, B. P. *Numerical Recipes in Fortran*; Cambridge University Press: New York, 1992.
(26) Chandler, D. *Introduction to Modern Statistical Mechanics*; Oxford University Press: New York, 1987.
(27) Baer, T.; Hase, W. L. *Unimolecular Reaction Dynamics: Theory and Experiments*; Oxford University Press: New York, 1996.
(28) Kindt, J. T.; Tully, J. C.; Head-Gordon, M.; Gomez, M. A. *J. Chem. Phys.* **1998**, *109*, 3629.
(29) Doubleday: C.; Li, G.; Hase, W. L. *Phys. Chem. Chem. Phys.* **2002**, *4*, 304.
(30) Ichiye, T.; Karplus, M. *Proteins* **1991**, *11*, 205.
(31) Danailov, D. M.; Yan, T.; Hase, W. L., work in progress, 2003.